

# Real-Time 4x3.5 Gbps Sigma Delta Radio-over-Fiber for a Low-Cost 5G C-RAN Downlink

Chia-Yi Wu, Haolin Li, Joris Van Kerrebrouck, Laurens Breyne, Laurens Bogaert, Piet Demeester, and Guy Torfs

IDLab, INTEC, Ghent University - imec, Ghent, Belgium, [ChiaYi.Wu@UGent.be](mailto:ChiaYi.Wu@UGent.be)

**Abstract** A 4-lane proof-of-concept real-time sigma-delta-over-fiber system targeting 5G C-RAN downlink is demonstrated using off-the-shelf components. Per lane, an EVM of 2.67% is achieved for a 3.5 Gbps 256-QAM signal modulated at 3.5 GHz over 20-km single-mode fiber at 1310 nm.

## Introduction

The upcoming fifth generation (5G) cellular network demands massive device connectivity, high data rate, decreased latency and sustainable cost<sup>1</sup>. To achieve the challenging goals, the centralized/cloud radio access network (C-RAN) architecture is one of the key enablers<sup>2</sup>. In 5G C-RAN, a central office (CO) should be able to control hundreds or even thousands of remote radio heads (RRHs) via the fronthaul network<sup>3</sup>. The centralized processing allows resource-sharing at the CO. It also provides the possibility to use cooperative radio technologies to reduce the interference between RRHs, allowing an increase in the RRH density.

The fronthaul network is expected to meet the high-capacity and low-latency requirements. To deploy a large number of cells, the critical aspects are cost, complexity and power consumption of the RRH. Considering these factors comprehensively, the radio-over-fiber (RoF) technologies are the most convincing candidates for the fronthaul network<sup>3</sup>.

Various RoF schemes exist; each has its own RRH implementation as shown in Fig. 1. Digitized radio-over-fiber (DRoF) links using CPRI<sup>4</sup> or OBSAI<sup>5</sup> are common in today's traditional macro-cellular wireless communications<sup>6</sup>. Despite the largest advantage of DRoF—immunity to nonlinearities, DRoF is not a good option due to its low bandwidth efficiency<sup>3</sup> and RRH complexity as shown in Fig. 1a. The cost and power consumption of the digital-to-analog converter (DAC) at the RRH can be considerable for high baud rates. Because the RRH receives baseband signals, an up-converter is mandatory at the RRH.

Analog radio-over-fiber (ARoF), illustrated in Fig. 1b, is proposed in favor of its simple RRH architecture. At the CO, the signal is converted to an analog signal at the carrier frequency and

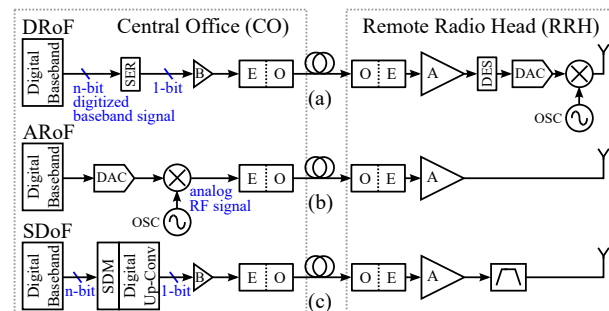


**Fig. 1:** Example of a (a) DRoF, (b) ARoF and (c) SDoF link. E-O: electrical-to-optical; O-E: optical-to-electrical; SER: serializer; DES: de-serializer; B: binary driver; A: amplifier; OSC: oscillator; SDM: sigma delta modulator.

transmitted over fiber. Hence, the RRH needs no DAC and frequency conversion. Yet ARoF is vulnerable to nonlinearities; this results in stringent requirements for analog electronic devices and optical transmitters.

An alternative approach is transmitting a sigma delta modulated signal over fiber (SDoF) (Fig. 1c). A sigma delta modulator (SDM)<sup>7</sup> oversamples the baseband signal and quantizes it to a 1-bit signal. A digital up-converter moves the signal to the required center frequency. A properly designed band-pass filter (BPF) eliminates the out-of-band quantization noise shaped by the SDM and guarantees that the spectral mask requirements are met.

SDoF combines the advantages of DRoF and ARoF. Like DRoF, it is immune to nonlinearities. The requirements of analog devices are relaxed and it is possible to use non-linear direct-modulated laser sources<sup>8</sup>. The simple and power-efficient RRH can also be used for ARoF.

This paper presents a real-time demonstration of a 4x3.5 Gbps SDoF link with 3.5 GHz center frequency at 850 nm and 1310 nm using commercial off-the-shelf components. The system architecture, measurement setup and results are provided in the following sections.

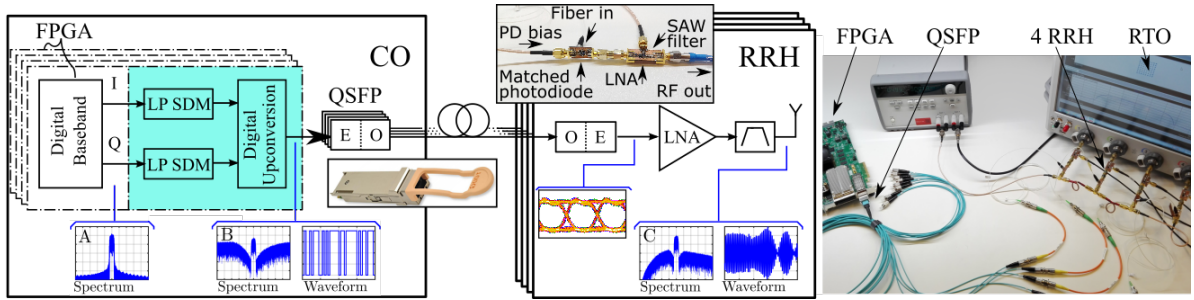


**Fig. 2:** Block diagram, measurement setup and the illustrated waveforms and spectra: A: the digital baseband I/Q signal; B: the signal modulated by the SDM and up-converted by the digital up-converter; C: the signal after the band-pass filter at the RRH.

## System Architecture

Fig. 2 shows the block diagram of the 4 SDoF links in which 4 pairs of in-phase (I) and quadrature (Q) baseband signals are modulated by 4x2 high-speed second-order low-pass SDMs (LP SDMs) at 7 GSps (sample per second). Second-order LP SDMs are chosen for this architecture to have a high signal-to-noise and distortion ratio (SNDR) notwithstanding the complexity and design difficulty. To achieve the desired sample rate, a parallel multi-stage scheme is applied<sup>9</sup>. The quantization noise is shaped by the LP SDMs to higher frequencies, i.e. out of the band of interest.

A digital upconversion<sup>10</sup> is used to translate the modulated I and Q signal (both 1-bit) to one 14 Gbps binary signal at the center frequency of 3.5 GHz, followed by the subsequent electrical-optical conversion. The optical signals are transmitted over multi-mode fibers (MMFs) or single-mode fibers (SMFs). At each RRH, the photodiode of the receiver is impedance-matched to the low-noise amplifier (LNA) to maximize the power transfer at 3.5 GHz<sup>11</sup>; the LNA amplifies the electrical signal coming from the photodiode. After the LNA, the quantization noise is filtered by a BPF.

## Measurement Setup

The digital baseband generators, LP SDMs and digital up-converters, shown in Fig. 2, are implemented on a *Xilinx Virtex Ultrascale* FPGA (VCU108). For the electrical-optical conversion, we use a QSFP-100G-SR4 (850 nm) module to transmit over OM4 MMFs and a QSFP-100G-PSM4 (1310 nm) for SMFs. Each module consists of 4 parallel transmitters; each transmitter has a clock and data recovery (CDR) block to resample the data, a laser driver and a VCSEL (vertical-cavity surface-emitting laser)/DFB (distributed feedback laser). An MTP/MPO breakout fiber carries the 4 light streams into 4 individual fibers for different RRHs. The photo receivers use *Mini-Circuits* amplifiers PMA3-83LN+ to amplify the electrical signals coming from the

photodiodes. The out-of-band noise is eliminated by BPFs. Instead of transmitting the signals with antennas, a real-time oscilloscope (RTO) (DSAZ634A) is used for demodulation to evaluate the signal quality.

## Measurement Results

Single-carrier 256-QAM modulated signals are transmitted over SDoF links. The performance is evaluated for various symbol rates—87.5, 218.75 and 437.5 MBd—and different fiber lengths—200 m OM4 MMF and 2 km, 5 km and 20 km SMF. Optical back-to-back (B2B) transmissions are also measured as the performance reference.

Fig. 3 shows the measured spectra of a B2B single-mode link at the output of the LNA. The noise-shaping performance of the SDM can be observed. Even though the outer edges of the spectra show lower signal-to-noise ratios (SNRs), the noise around the carrier frequency 3.5 GHz is much lower, resulting in good in-band SNRs.

The error vector magnitudes (EVMs), normalized to the constellation maximum, are measured as a function of different symbol rates and shown in Fig. 4. In the B2B cases, the single-mode link outperforms the multi-mode link (0.87% v.s. 1.21%). The EVMs increase accordingly with the symbol rates since the oversampling ratios decrease and the in-band quantization noise increases with 40 dB/dec given the fixed sample

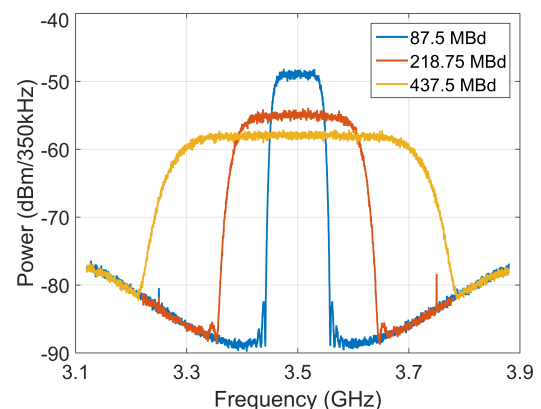


**Fig. 3:** Measured spectra at the RRH after the LNA.

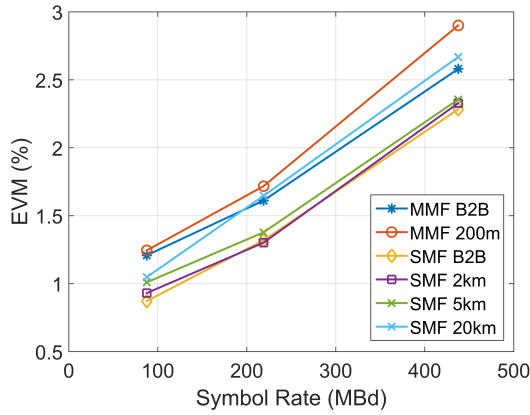


Fig. 4: Measured EVM for multi-mode and single-mode links.

rate used.

For both multi-mode and single-mode links, a small degradation in EVM is observed for longer fiber lengths. For the 20 km single-mode link, the performance seems to degrade faster than others. The main reason is that the received signal power is low due to the path loss while the thermal noise and the noise caused by the LNA remain the same. Nevertheless, the 2.67% EVM of the 437.5 MBd signal is sufficiently low to receive a 256-QAM modulated signal, yielding a 3.5 Gbps throughput per link.

Fig. 5 shows the demodulated constellation diagrams. The diagram Fig. 5a is obtained after the B2B transmission of an 87.5 MBd signal and Fig. 5b shows the constellation diagram when a 437.5 MBd signal is transmitted over 20 km SMF.

For short-range applications<sup>12</sup>, the multi-mode link is a low-cost solution. The measurement results of single-mode links confirm that SDoF can be used for 5G C-RAN, which expects up to 10 km transmission distance over fiber<sup>2</sup>. Furthermore, it can provide backward compatibility with 4G C-RAN, whose maximum distance between COs and RRHs is within 20-40 km<sup>6</sup>.

## Conclusions

In this paper, we demonstrate a real-time 4x3.5 Gbps sigma-delta-over-fiber link with 3.5 GHz center frequency at 850 nm and 1310 nm using off-the-shelf components. The 14 GSps sigma delta modulators are implemented on FPGA. The architecture can be applied to the 5G sub-6GHz band. The measurement results show an EVM of 2.67% for a 3.5 Gbps (437.5 MBd 256-QAM modulated) signal transmitted over 20 km single-mode fiber using DFB. The performance corroborates that sigma-delta-over-fiber can cover the desired range of the 5G C-RAN fronthaul networks and can even be backward

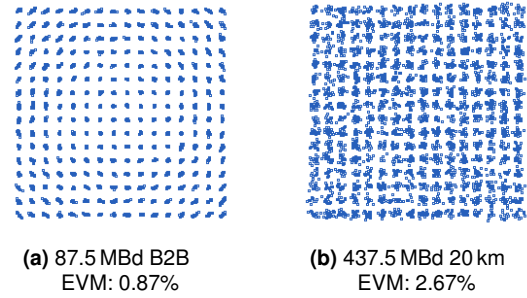


Fig. 5: Constellation diagrams for single-mode links.

compatible with 4G C-RAN while having low-complexity, low-cost and low-power remote radio heads.

## Acknowledgements

This work was supported by the ERC Advanced Grant ATTO project (No. 695495) and H2020 5G-PHOS project (No. 761989).

## References

- [1] A. Gupta et al., "A Survey of 5G Network: Architecture and Emerging Technologies," *IEEE Access*, Vol. **3**, p. 1206-1232 (2015).
- [2] China Mobile Research Institute, Beijing, China, "C-RAN: the Road Towards Green RAN," White Paper (2013).
- [3] C. Ranaweera et al., "5G C-RAN with Optical Fronthaul: an Analysis from a Deployment Perspective," *J. Lightw. Technol.*, Vol. **36**, no. 11, p. 2059-2068 (2018).
- [4] Common Public Radio Interface (CPRI) [Online] (Available: <http://www.cpri.info/>).
- [5] Open Base Station Architecture Initiative (OBSAI) [Online] (Available: <http://www.obsai.com/>).
- [6] A. Checko et al., "Cloud RAN for Mobile Networks—a Technology Overview," *Commun. Surveys Tuts.*, Vol. **17**, no. 1, p. 405-426 (2015).
- [7] M. Ebrahimi et al., "Delta-Sigma-Based Transmitters: Advantages and Disadvantages," *IEEE Microw. Mag.*, Vol. **14**, p. 66-78 (2013).
- [8] L. Breyne et al., "Comparison Between Analog Radio-Over-Fiber and Sigma Delta Modulated Radio-Over-Fiber," *IEEE Photon. Technol. Lett.*, Vol. **29**, no. 21, p. 1808-1811 (2017).
- [9] R. Hossain et al., "Parallel MASH  $\Delta\Sigma$  modulator," US Patent US8203475B2 [Online] (Available: <https://patents.google.com/patent/US8203475>) (2012).
- [10] A. Frappe et al., "An All-Digital RF Signal Generator Using High-Speed  $\Delta\Sigma$  Modulators," *IEEE J. Solid-State Circuits*, Vol. **44**, no. 10, p. 2722-2732 (2009).
- [11] J. Van Kerrebrouck et al., "Real-Time All-Digital Radio-over-Fiber LTE Transmission," *Advances in Wireless and Optical Communications*, p. 83-86 (2017).
- [12] G. Torfs et al., "ATTO: Wireless Networking at Fiber Speed," *J. Lightw. Technol.*, Vol. **36**, no. 8, p. 1468-1477 (2018).